Focal adhesion kinase confers pro-migratory and anti-apoptotic properties and is a potential therapeutic target in Ewing sarcoma

Running title: Focal adhesion kinase in Ewing sarcoma

Konrad Steinestel[1,2]*, Esther-Pia Jansen[1], Marcel Trautmann[1,3], Uta Dirksen[4], Jan Rehkämper[1], Jan-Henrik Mikesch[5], Julia S. Gerke[6], Martin F. Orth[6], Giuseppina Sannino[6], Eva Wardelmann[1], Thomas G. P. Grünewald[6,7,8,9], Wolfgang Hartmann[1,3]

[1]Gerhard Domagk Institute of Pathology, University Hospital Münster, Münster, Germany
[2]Institute of Pathology and Molecular Pathology, Bundeswehrkrankenhaus Ulm, Ulm, Germany
[3]Division of Translational Pathology, Gerhard-Domagk-Institute of Pathology, University Hospital Münster, Münster, Germany
[4]Pediatrics III, West German Cancer Centre, University Hospital Essen, Essen, Germany
[5]Department of Medicine A, University Hospital Münster, Münster, Germany
[6]Max Eder Research Group for Pediatric Sarcoma Biology, Institute of Pathology, Faculty of Medicine, LMU Munich, Munich, Germany
[7]German Cancer Consortium (DKTK), partner site Munich, Munich, Germany
[8]German Cancer Research Center (DKFZ), Heidelberg, Germany
[9]Institute of Pathology, Faculty of Medicine, LMU Munich, Munich, Germany

***corresponding author**

Konrad Steinestel, MD PhD
Institute of Pathology and Molecular Pathology
Bundeswehrkrankenhaus Ulm
Oberer Eselsberg 40
89081 Ulm, Germany

Phone: 0049 731 1710 2400
Fax: 0049 731 1710 2403

E-mail: konrad@steinestel.com

Competing Interests Statement

This work has been funded by the Deutsche Forschungsgemeinschaft (DFG) grant no. STE 2467/1-1 (to KS) and the Wilhelm Sander-Stiftung grant no. 2016.099.1 (to WH, MT and KS). The laboratory of TGPG is supported by grants from the German Cancer Aid (DKH-111886 and DKH-70112257).

ABSTRACT

Oncogenesis of Ewing sarcoma (EwS), the second most common malignant bone tumor of childhood and adolescence, is dependent on the expression of chimeric EWSR1-ETS fusion oncogenes, most often EWSR1-FLI1 (E/F).

E/F expression leads to dysregulation of focal adhesions (FAs) enhancing the migratory capacity of EwS cells. Here we show that, in EwS cell lines and tissue samples, focal adhesion kinase (FAK) is expressed and phosphorylated at Y397 in an E/F-dependent way involving Ezrin. Employing different EwS cell as *in vitro* models, we found that key malignant properties of E/F are mediated via substrate-independent autophosphorylation of FAK on Y397. This phosphorylation results in enhanced FA formation, Rho-dependent cell migration, and impaired caspase-3-mediated apoptosis *in vitro*. Conversely, treatment with the FAK inhibitor Y15 enhanced caspase-mediated apoptosis and EwS cell migration, independent from the respective EWSR1-ETS fusion type, mimicking an anoikis-like phenotype. Our findings were confirmed *in vivo* using an avian chorioallantoic membrane (CAM) model. Our results provide a first rationale for the therapeutic use of FAK inhibitors to impair metastatic dissemination of EwS.

KEYWORDS

Ewing sarcoma; focal adhesion kinase; cytoskeleton; migration; metastasis

INTRODUCTION

Ewing sarcoma (EwS) is a highly aggressive cancer of bone and soft tissue that predominantly affects children and adolescents. Frequently, (micro-)metastasis is already present at the time of diagnosis, and no effective therapy strategies have been established for these patients yet [6, 33]. Knowledge of the biological mechanisms underlying EwS cell migration might provide rationales for developing urgently needed targeted therapies to prevent or to slow down metastatic dissemination of EwS cells.

EwS are genetically stable tumors characterized by a chromosomal translocation leading to fusion of the *EWSR1* gene on chromosome 22 and variable members of the ETS family of transcription factors. In 85% of cases, the translocation partner for *EWSR1* is *FLI1* on chromosome 11; other possible fusion partners are, among others, the *ERG, FEV* or *ETV1/4* genes [19, 26]. The resulting chimeric transcription factor *EWSR1-FLI1* (E/F) modulates the expression of a large number of target genes, leading to oncogenic transformation of the cell harboring this fusion [1].

So far, only a few studies have investigated the effect of E/F expression on cell migration and invasion of EwS cells as a prerequisite to metastasis. Using an RNA interference approach, Chaturvedi *et al.* demonstrated that knockdown of E/F enhanced tumor cell adhesion and spreading; in a subsequent study, the same group showed that E/F-induced repression of Zyxin and α5 integrin impairs cell adhesion and actin cytoskeletal integrity, thus supporting anchorage-independent cell growth [3, 4]. CXCR4-dependent migration and invasion of EwS cells were shown to depend on the activity of small Rho-GTPases RAC and CDC42 [16].

Focal adhesion kinase (FAK) is a substrate of SRC kinase and localizes to focal adhesions (FAs), where it is activated by integrins, resulting in FA reorganization and increased cell motility [20]. Integrin-mediated autophosphorylation of FAK on Y397 inhibits detachment-dependent apoptosis, a process named anoikis [7]. There is experimental evidence that autophosphorylation of FAK on Y397 results from dimerization of two FAK molecules [32]. Alternatively, FAK autophosphorylation can be induced by the FAK interaction partner Ezrin independent from cell-matrix adhesion [22]. Ectopic expression of constitutively active FAK rescues cancer cells from induced anoikis [7]. Moreover, FAK activation appears to be essential for migration as well as mechano-induced osteogenic differentiation of mesenchymal stem cells (MSCs) that are believed to constitute the cells of origin in EwS [25, 27, 34]. One report previously identified FAK as a potential therapeutic target in EwS by the use of high-throughput tyrosine kinase activity profiling [5]. In line, another report showed that miR-138, via

102 targeting *FAK*, inhibits proliferation and mobility and induces anoikis of EwS cells [31]. However, the
103 exact role of FAK in EwS remains elusive.

104

105 Here, we show that E/F-dependent autophosphorylation of FAK is a crucial mechanism underlying
106 EwS aggressivity as it promotes a migratory phenotype and inhibits caspase-mediated apoptosis. We
107 show that this mechanism can effectively be targeted by the FAK inhibitor Y15, independent from the
108 respective *EWSR1-ETS* fusion type. Hence, our results point toward a possible use of FAK inhibitors to
109 prevent metastatic dissemination in EwS.

110 **RESULTS AND DISCUSSION**

111 **Doxycycline (DOX)-inducible downregulation of *EWSR1-FLI-1* (E/F) attenuates Ezrin expression and**
112 **Y397-phosphorylation of FAK in A673 EwS cells.**

113 In order to investigate E/F-dependent changes in FA gene expression levels, a DOX-inducible E/F
114 knockdown in A673 EwS cells was performed, revealing decreased levels of *Ezrin* mRNA upon E/F
115 knockdown (Fig. 1 A). Ezrin has previously been shown to induce FAK autophosphorylation
116 independent from SRC signaling and FAK/integrin interaction[22]. Correspondingly,
117 immunohistochemical analyses of xenograft tumors derived from A673 cells showed significantly
118 decreased Ezrin protein expression and Y397-phosphorylation of FAK upon loss of E/F while total FAK
119 protein expression was unaffected (Fig. 1 B). These findings are in line with previous results showing
120 i) strong expression of Ezrin in primary EwS samples and ii) experimental data supporting a central
121 role of Ezrin in both autophosphorylation of FAK and growth and metastatic spread of EwS[15, 22].

122 **Y397-phosphorylation of FAK in EwS cells depends on the presence of Ezrin**

123 For further *in vitro* studies, we employed the EwS cell lines A673, TC-32 (both EWSR1-FLI1 fusion
124 type 1) and CADO-ES1 (EWSR1-ERG fusion gene) (Supplementary Fig. 1) [18, 29]. All EwS cell lines
125 strongly expressed Ezrin (Supplementary Fig. 1 E). siRNA-based knockdown of Ezrin significantly
126 impaired Y397-phosphorylation of FAK in A673 (Fig. 1C), TC-32 and CADO-ES1 cells (Supplementary
127 Figure 1 B). Notably, in CADO-ES1 cells, the effect on Y397-phosphorylation was limited to one Ezrin
128 siRNA (#3) and could only be observed 72h after transfection. Taken together, these findings suggest
129 a model in which FAK autophosphorylation in EwS occurs dependent on E/F-driven Ezrin expression.

130 **FAK is ubiquitously expressed and phosphorylated at Y397 in Ezrin-positive EwS tumor samples.**

131 To investigate the relevance of our *in vitro* and *ex vivo* findings in patients, immunohistochemical
132 analyses were performed in a set of tumor samples homogeneously treated in the EWING99 trial

(*n*=93; Fig. 1 D; Supplementary Table 1). All investigated samples showed moderate to strong FAK staining with Ezrin being expressed in 79% of tumors. Phosphorylated FAK (Y397) was detected in 78% of samples, which were all simultaneously Ezrin-positive ($p<0.0001$, Chi-square test). Surprisingly, there was no significant correlation between FAK expression levels, Ezrin expression, or phosphorylation of FAK and clinicopathological characteristics, such as response to chemotherapy, first relapse or presence of metastatic disease at the time of diagnosis. This lack of clinical association may well be due to the fact that a vast majority of samples in our cohort were Ezrin/pFAK double-positive (79% and 78%, respectively). However, in concordance with our results, Krishnan *et al.*, investigating a similar percentage of strongly Ezrin-positive EwS samples, found no significant differences in the "ezrin score" of patients with localized versus metastatic disease[15]. Thus, the biological impact of Ezrin on the course and outcome of EwS remains to be elucidated as it might be masked by possible alternative signaling pathways in Ezrin-negative EwS.

EwS cell lines show adhesion- and fusion type-independent Y397-phosphorylation of FAK that can be targeted by 1,2,4,5-Benzenetetraamine tetrahydrochloride (FAK inhibitor 14, Y15).

A673, TC-32 and CADO-ES1 remained viable and showed enhanced FAK phosphorylation when grown under non-adherent conditions (Fig. 2 A), which is of special interest since it had previously been shown that Y397-phosphorylation of FAK inhibits anoikis (detachment-dependent apoptosis)[7]. The compounds PF-573228 (PF-228) and Y15 are potent and specific inhibitors of FAK autophosphorylation activity[9, 28]. Y15 has previously been shown to decrease cell viability and clonogenicity of various carcinomas and to increase detachment, cause apoptosis and inhibit invasion of glioblastoma cells through the inhibition of FAK [10, 35]. We could confirm that both Y15 and PF-228 (data not shown) abrogate Y397-phosphorylation of FAK in EwS; we selected Y15 for further experiments since its *in vivo* activity has already been documented [12]. Application of 10 µmol/l Y15 effectively impaired FAK phosphorylation in all three cell lines (Fig. 2 B). The decrease in FAK phosphorylation upon Y15 treatment occurred in parallel with an increase in caspase-3 cleavage and apoptosis as shown by immunoblotting and ApoTox Glo Triplex assays. Fluorescence microscopy and image analysis revealed a significant decrease in the number and size of focal adhesions together with a loss of dorsal actin stress fibers (Fig. 2 C). The decrease in FA formation together with increased caspase 3-mediated apoptosis points towards enhanced anoikis in Y15-treated EwS cells, given that caspase 3 is one of the key effector molecules of detachment-dependent cell death[8]. Moreover, application of 10 µmol/l Y15 significantly impaired cell migration of A673, TC-32 and CADO-ES1 in real-time cell migration assays (Fig. 2 D) together with a decrease in active Rho levels as shown by Rho activity pulldown assays (Fig. 2 E). Since FAK has previously been identified as a potential therapeutic target in EwS, and since migration and invasion of EwS depend on the activity

of small Rho-GTPases[5, 16], these findings support a potential therapeutic role of FAK inhibition in prevention or slowing down metastatic dissemination of EwS.

Y15 impairs viability and invasion of EwS in an *in vivo* (avian CAM) model.

A chicken chorioallantoic membrane (CAM) model was used to assess the effects of Y15 on EwS tumor xenografts *in vivo*. Application of 10 µmol/l Y15 alone did not have morphologic effects, particularly with regard to the microvascular architecture of the CAM (Fig. 3 A). However, treatment of A673 cells with 10 µmol/l Y15 prior to cell seeding significantly impaired tumor formation (p=0.0122) and led to a significant decrease in the size of invasive experimental EwS (p=0.0095) along with widespread tumor regression, necrosis and microcalcification with only few residual tumor cell clusters (Fig. 3 B). Immunohistochemistry showed expression of FAK in both, Y15-treated and control cells, but barely detectable Y397-phosphorylation of FAK in the few residual tumor cells after Y15-treatment (p<0.001).

In summary, the findings presented here lead to a model where *EWSR1-ETS*-dependent expression of Ezrin leads to SRC-independent autophosphorylation of FAK on tyrosine 397 that impairs apoptosis/anoikis and enhances focal adhesion formation as well as Rho-dependent cell migration of EwS cells (Fig. 3 C). This pathway can be effectively targeted by application of the FAK inhibitor Y15.

Our results show that key tumorigenic properties of EwS cells depend on Y397-autophosphorylation of FAK, further underlining the crucial role of FA homeostasis in cancer cells, [30] and a possible role of FAK inhibitors in treatment of EwS. The effects of FAK inhibition were independent from the underlying *EWSR1-ETS* fusion gene. It is well conceivable that autophosphorylation of FAK depends on the structural integrity of the FA protein complex, whose components, such as Ezrin, underlie direct transcriptional control by the E/F oncogene. While further studies should aim at deciphering the exact way how expression of the oncogenic transcription factor affects FA protein composition in EwS cells, the present work clearly identified FAK autophosphorylation as a potential therapeutic target affecting metastatic dissemination in EwS.

MATERIALS AND METHODS

DOX-inducible knockdown and *in vivo* xenografts

A673/TR/shEF1 cells[2], which contain a doxycycline (DOX)-inducible shRNA against *EWSR1-FLI1*, were injected subcutaneously in the flanks of immunocompromised NSG (NOD/scid/gamma) mice. When tumors reached an average volume of 180 mm^3, mice were randomized and either received 2 mg/ml DOX (Sigma) and 5% sucrose in the drinking water (DOX +) or only 5% sucrose (DOX –). Mice were sacrificed after 96h, and tumors were isolated for RNA and histological analysis. RNA was extracted

199 using the ReliaPrep miRNA Cell and Tissue Miniprep System (Promega). Knockdown of *EWSR1-FLI1*
200 was confirmed by qRT-PCR[11]. The transcriptome of each tumor (*n*=3 for DOX+ and DOX–) was
201 profiled on Affymetrix Clariom D arrays (RIN>9). Microarray data were normalized on gene level
202 using Signal Space Transformation Robust Multi-Chip Average (SST-RMA) and Affymetrix CDF. Three
203 FFPE cores (1 mm) were taken from each xenograft tumor to create a tissue microarray (TMA).
204 Animal experiments were conducted in accordance with the recommendations of the European
205 Community (86/609/EEC), the Government of Upper Bavaria (Germany), and UKCCCR (guidelines for
206 the welfare and use of animals in cancer research).

207 **Immunohistochemistry of EwS patient samples**

208 Immunohistochemistry was performed on TMA slides containing at least two representative cores (1
209 mm) derived from a FFPE tissue samples from 97 EwS patients from the cooperative Ewing sarcoma
210 study (CESS) group with full clinical and follow-up information; clinico-pathological data are given in
211 Supplementary Table 1. TMAs were stained using anti-FAK/phospho-FAK/Ezrin antibodies (1:1000;
212 Cell signaling, Frankfurt, Germany). Immunohistochemical staining was graded as strong (2; intense
213 staining in ≥50% of tumor cells), moderate (1; intermediate to intense staining in 1-49% of tumor
214 cells), and negative (0, no staining or staining in <1% of tumor cells). Software-based quantification
215 was performed with the reciprocal intensity method (ImageJ, NIH, Maryland, USA)[21].

216 **Cell lines and cell-based analyses**

217 A673, TC-32 (EWSR1-FLI1 translocated) and CADO-ES1 (EWSR1-ERG translocated) cells have been
218 described before[14, 18, 19, 24]. Cells were grown in DMEM with 10% fetal bovine serum (FBS) and RPMI
219 medium with 15% FBS, respectively. All cell lines were authenticated using STR analysis (data not
220 shown). For cultivation under adhesion-free conditions, we used Softwell AF adhesion-free hydrogel
221 plates (#SW6-AF; Matrigen Technologies, USA).

222 *Western immunoblotting*

223 Western blotting was performed using a routine protocol after cell lysis in RIPA buffer including
224 protease and phosphatase inhibitors (#9806 and #5872 Cell signaling, Frankfurt, Germany). Grayscale
225 intensity values were normalized to internal positive controls and measured using ImageJ software
226 (NIH, Maryland, USA).

227 *siRNA knockdown*

228 A673, TC-32 and CADO-ES1 Ewing sarcoma cells were grown in 25 cm^2 cell culture flasks (medium
229 supplemented with 2% FBS) and transfected with indicated siRNA (25 pmol; cell density of 50%) using
230 Lipofectamine RNAiMAX (Life Technologies). A set of pre-validated short interfering RNA (Silencer

Select siRNA, Life Technologies) targeting EZR (Entrez Gene ID 7430) was used: #2 (ID s14796) = sense: 5′-GGCUUUCCUUGGAGUGAAAtt-3′; antisense: 5′-UUUCACUCCAAGGAAAGCCaa-3′ and #3 (ID s14797) = sense: 5′- GGAAUCAACUAUUUCGAGAtt -3′; antisense: 5′-UUUCACUCCAAGGAAAGCCaa-3′. Non-targeting control siRNA (BLOCK-iT Alexa Fluor Red Fluorescent Control, Life Technologies) was included to screen for unspecific off-target effects. After incubation for 48-72 hours, siRNA-transfected cells were lysed and knockdown efficiency was documented by Western immunoblotting.

xCelligence system

The xCelligence system (OLS, Bremen, Germany) was used for real-time, label-free monitoring of cell health and behavior. Cells were seeded on E-Plate 16 (cell proliferation and adhesion) or into the upper chamber of CIM-Plate 16 (cell migration). Cell proliferation, morphology change, and attachment quality was measured using electrical impedance; cell migration was monitored using the electronically integrated Boyden chamber of CIM-Plate 16 with 10% FBS as chemoattractant in the lower chamber. All experiments were performed in quadruplicate using both 20,000 and 40,000 cells for each experimental condition.

Immunofluorescence (IF) microscopy and focal adhesion (FA) quantification and measurement

IF staining was performed as previously described[17]. The number of FAs was quantified using ImageJ (NIH, Maryland, USA) following a published protocol with slight modifications[23]. In short, (1) 30 randomly selected cells were photographed, (2) channels were split, (2) outlines of Paxillin-positive FAs were detected, (3) objects meeting the predefined criteria for FAs (size, circularity) were counted automatically for each cell. The number of FAs was normalized to the respective cell area. FA diameter was measured using the measurement tool of ImageJ.

ApoTox-Glo® assay

The ApoTox-Glo® Assay (Promega, Mannheim, Germany) was used following the manufacturer's protocol. A673 EwS cells were treated with Y15 (10 µmol/l) or volume-adapted concentrations of DMSO for 24h. Free AFC as a marker of viable cells was determined by measurement of fluorescence at 400 nm excitation/505 nm emission wavelengths; free R110 as a marker of necrotic cells was measured at 485 nm excitation/520 nm emission. Thirty minutes after adding Caspase-Glo® 3/7-reagent, the release of aminoluciferin was measured using a luminometer. All tests were performed in triplicate and normalized to control (background), vehicle (DMSO) and Y15 compound controls.

Rho activity assay

Rho activity was assessed using the Rho Activity assay from Cell Signaling (#8820, Cell Signaling, Frankfurt, Germany). GTPase activity was measured based on the ability of the GTP-bound (active) form of Rho to bind Rhotekin-RBD fusion protein; this was then immunoprecipitated with glutathione resin. The level of Rho as detected in subsequent Western immunoblotting correlates with its activation state.

Reagents

Y15 (1,2,4,5-Benzenetetraamine tetrahydrochloride; FAK Inhibitor 14, Cat. No. 3414) was obtained in pharmaceutical purity from Tocris Bioscience (Bristol, UK).

Chorioallantoic membrane (CAM) model

CAM assays were performed as previously described[13]. Fertilized eggs of White Leghorn chickens were incubated at 37°C with 60% relative humidity and prepared for implantation on day 4 of incubation. Each egg was washed with warm 70% ethanol and a hole was drilled through the pointed pole of the shell. The following day, the chorioallantoic membrane was exposed by peeling a 1.5–2.0 cm window in the shell. This window was covered with tape and the incubation continued. On day 8 of incubation, DMSO/Y15-treated A673 EwS cells were dissolved in Matrigel and introduced in the CAM. Tumor growth was assessed macroscopically during the following days. After 5 days, tumors were harvested, measured and weighed, fixed in 5% PFA and processed for histopathological examination with H/E, FAK/pFAK (Y397) and Ezrin staining as described above.

Statistical analyses

Survival analyses (Kaplan-Meier method) for the patient-derived sample cohorts were done with SPSS (IBM, Mannheim, Germany). All statistical analyses for the *in vitro* data were performed using GraphPad software (GraphPad, LaJolla, USA). We used Chi-Square/Fisher's exact test for the comparison of categorical variables, while student's t-test/ANOVA followed by Tukey's multiple comparison test was performed to compare continuous variables between two groups/more than two groups, respectively. A p value <0.05 was regarded as statistically significant.

REFERENCES

1 Braun BS, Frieden R, Lessnick SL, May WA, Denny CT. Identification of target genes for the Ewing's sarcoma EWS/FLI fusion protein by representational difference analysis. Molecular and Cellular Biology 1995; 15: 4623-4630.

2 Carrillo J, García-Aragoncillo E, Azorín D, Agra N, Sastre A, González-Mediero I *et al*. Cholecystokinin down-regulation by RNA interference impairs Ewing tumor growth. Clinical Cancer Research 2007; 13: 2429-2440.

3 Chaturvedi A, Hoffman LM, Welm AL, Lessnick SL, Beckerle MC. The EWS/FLI oncogene drives changes in cellular morphology, adhesion, and migration in Ewing sarcoma. Genes & cancer 2012; 3: 102-116.

4 Chaturvedi A, Hoffman LM, Jensen CC, Lin Y-C, Grossmann AH, Randall RL *et al*. Molecular dissection of the mechanism by which EWS/FLI expression compromises actin cytoskeletal integrity and cell adhesion in Ewing sarcoma. Molecular biology of the cell 2014; 25: 2695-2709.

5 Crompton BD, Carlton AL, Thorner AR, Christie AL, Du J, Calicchio ML *et al*. High-throughput tyrosine kinase activity profiling identifies FAK as a candidate therapeutic target in Ewing sarcoma. Cancer research 2013; 73: 2873-2883.

6 Dahlin DC, Coventry MB, Scanlon PW. Ewing's Sarcoma: A Critical Analysis of 165 Cases. JBJS 1961; 43: 185-192.

7 Frisch SM, Vuori K, Ruoslahti E, Chan-Hui P-Y. Control of adhesion-dependent cell survival by focal adhesion kinase. The Journal of cell biology 1996; 134: 793-799.

8 Frisch SM, Screaton RA. Anoikis mechanisms. Current opinion in cell biology 2001; 13: 555-562.

9 Golubovskaya V, Curtin L, Groman A, Sexton S, Cance WG. In vivo toxicity, metabolism and pharmacokinetic properties of FAK inhibitor 14 or Y15 (1, 2, 4, 5-benzenetetramine tetrahydrochloride). Archives of toxicology 2015; 89: 1095-1101.

10 Golubovskaya VM, Huang G, Ho B, Yemma M, Morrison CD, Lee J *et al*. Pharmacologic blockade of FAK autophosphorylation decreases human glioblastoma tumor growth and synergizes with temozolomide. Molecular cancer therapeutics 2013; 12: 162-172.

11 Grünewald TG, Bernard V, Gilardi-Hebenstreit P, Raynal V, Surdez D, Aynaud M-M *et al*. Chimeric EWSR1-FLI1 regulates the Ewing sarcoma susceptibility gene EGR2 via a GGAA microsatellite. Nature genetics 2015; 47: 1073.

12 Hochwald SN, Nyberg C, Zheng M, Zheng D, Wood C, Massoll NA *et al*. A novel small molecule inhibitor of FAK decreases growth of human pancreatic cancer. Cell cycle 2009; 8: 2435-2443.

13 Isachenko V, Mallmann P, Petrunkina AM, Rahimi G, Nawroth F, Hancke K *et al*. Comparison of in vitro-and chorioallantoic membrane (CAM)-culture systems for cryopreserved medulla-contained human ovarian tissue. PloS one 2012; 7: e32549.

14 Kodama K, Higashiyama M, Yokouchi H, Tateishi R, Mori Y. Differentiation of a Ewing's sarcoma cell line towards neural and mesenchymal cell lineages. Cancer Science 1994; 85: 335-338.

15 Krishnan K, Bruce B, Hewitt S, Thomas D, Khanna C, Helman LJ. Ezrin mediates growth and survival in Ewing's sarcoma through the AKT/mTOR, but not the MAPK, signaling pathway. Clinical & experimental metastasis 2006; 23: 227-236.

16 Krook MA, Nicholls LA, Scannell CA, Chugh R, Thomas DG, Lawlor ER. Stress-induced CXCR4 promotes migration and invasion of ewing sarcoma. Molecular Cancer Research 2014; 12: 953-964.

17 Liebau S, Steinestel J, Linta L, Kleger A, Storch A, Schoen M *et al*. An SK3 channel/nWASP/Abi-1 complex is involved in early neurogenesis. PloS one 2011; 6: e18148.

18 Matsui Y, Chansky HA, Barahmand-Pour F, Zielinska-Kwiatkowska A, Tsumaki N, Myoui A *et al*. COL11A2 collagen gene transcription is differentially regulated by EWS/ERG sarcoma fusion protein and wild-type ERG. Journal of Biological Chemistry 2003; 278: 11369-11375.

19 May WA, Gishizky ML, Lessnick SL, Lunsford LB, Lewis BC, Delattre O *et al*. Ewing sarcoma 11; 22 translocation produces a chimeric transcription factor that requires the DNA-binding domain encoded by FLI1 for transformation. Proceedings of the National Academy of Sciences 1993; 90: 5752-5756.

20 Mitra SK, Hanson DA, Schlaepfer DD. Focal adhesion kinase: in command and control of cell motility. Nature reviews Molecular cell biology 2005; 6: 56-68.

21 Nguyen DH, Zhou T, Shu J, Mao J. Quantifying chromogen intensity in immunohistochemistry via reciprocal intensity. Cancer InCytes 2013; 2: 1-4.

22 Poullet P, Gautreau A, Kadaré G, Girault J-A, Louvard D, Arpin M. Ezrin interacts with focal adhesion kinase and induces its activation independently of cell-matrix adhesion. Journal of Biological Chemistry 2001; 276: 37686-37691.

23 Ramadhani D, Rahardjo T, Nurhayati S. Automated Measurement of Haemozoin (Malarial Pigment) Area in Liver Histology Using ImageJ 1.6. *Proceeding of 6th Electrical Power, Electronics Communication, Control and Informatics Seminar (EECCIS), Malang*, 2012.

24 Ren C, Ren T, Yang K, Wang S, Bao X, Zhang F *et al*. Inhibition of SOX2 induces cell apoptosis and G1/S arrest in Ewing's sarcoma through the PI3K/Akt pathway. Journal of experimental & clinical cancer research : CR 2016; 35: 44.

25 Riggi N, Suvà M-L, Suvà D, Cironi L, Provero P, Tercier S *et al*. EWS-FLI-1 expression triggers a Ewing's sarcoma initiation program in primary human mesenchymal stem cells. Cancer research 2008; 68: 2176-2185.

26 Sankar S, Lessnick SL. Promiscuous partnerships in Ewing's sarcoma. Cancer genetics 2011; 204: 351-365.

27 Shih YRV, Tseng KF, Lai HY, Lin CH, Lee OK. Matrix stiffness regulation of integrin-mediated mechanotransduction during osteogenic differentiation of human mesenchymal stem cells. Journal of Bone and Mineral Research 2011; 26: 730-738.

28 Slack-Davis JK, Martin KH, Tilghman RW, Iwanicki M, Ung EJ, Autry C *et al*. Cellular characterization of a novel focal adhesion kinase inhibitor. Journal of Biological Chemistry 2007; 282: 14845-14852.

29 Smith R, Owen LA, Trem DJ, Wong JS, Whangbo JS, Golub TR *et al*. Expression profiling of EWS/FLI identifies NKX2.2 as a critical target gene in Ewing's sarcoma. Cancer Cell 2006; 9: 405-416.

30 Sulzmaier FJ, Jean C, Schlaepfer DD. FAK in cancer: mechanistic findings and clinical applications. Nature Reviews Cancer 2014; 14: 598-610.

31 Tanaka K, Kawano M, Itonaga I, Iwasaki T, Miyazaki M, Ikeda S *et al*. Tumor suppressive microRNA-138 inhibits metastatic potential via the targeting of focal adhesion kinase in Ewing's sarcoma cells. International journal of oncology 2016; 48: 1135-1144.

32 Toutant M, Costa A, Studler J-M, Kadaré G, Carnaud M, Girault J-A. Alternative splicing controls the mechanisms of FAK autophosphorylation. Molecular and cellular biology 2002; 22: 7731-7743.

33 Wang C, Schulz MD. Ewing's sarcoma: A study of fifty cases treated at the Massachusetts General Hospital, 1930–1952 inclusive. New England Journal of Medicine 1953; 248: 571-576.

34 Wang H, Wang X, Qu J, Yue Q, Hu Yn, Zhang H. VEGF enhances the migration of MSCs in neural differentiation by regulating focal adhesion turnover. Journal of cellular physiology 2015; 230: 2728-2742.

35 Zhang H, Shao H, Golubovskaya VM, Chen H, Cance W, Adjei AA *et al*. Efficacy of focal adhesion kinase inhibition in non-small cell lung cancer with oncogenically activated MAPK pathways. Br J Cancer 2016; 115: 203-211.

Figure 1. EWSR1-FLI1-dependent Ezrin expression and FAK Y397-phosphorylation in an Ewing sarcoma (EwS) *in vivo* model and primary human tumor samples. A, DOX-inducible knockdown of EWSR1-FLI1 in A673 cells showed downregulation of FLI-1 and Ezrin mRNA levels in A673 EwS cells, while FAK levels remained unaffected. **B,** Immunohistochemistry confirmed the downregulation of Ezrin on protein level along with a decrease in Y397-phosphorylation of FAK in A673-derived xenografts while FAK protein levels remained unaltered. **C,** siRNA-based knockdown of Ezrin led to a significant decrease in Y397-phosphorylation of FAK in EwS cells. **D,** Immunohistochemical analyses of FAK/Ezrin expression and Y397-phosphorylation of FAK in tissue samples derived from 97 EwS patients treated in the cooperative Ewing sarcoma study (CESS) trial. All EwS tumor samples were positive for FAK protein in immunohistochemistry, and the majority of tumor samples showed moderate to strong expression of Ezrin and Y397-phosphorylation of FAK (79% and 78% of cases, respectively). All pFAK+ cases were Ezrin+. Survival analyses showed no significant association between Ezrin expression/ FAK phosphorylation and overall survival (p=0.3203 and 0.9438, respectively).

Figure 2. Y397-phosphorylation of FAK under different cell culture conditions and upon application of the FAK inhibitor 1,2,4,5-Benzenetetraamine tetrahydrochloride (Y15) A, In EwS cell lines grown under adherent and non-adherent conditions, Y397-phosphorylation of FAK was not only persistent, but increased under adhesion-free conditions in three different EwS cell lines (A673, TC-32 and CADO-ES1) as shown by Western immunoblotting and densitometric analysis. **B,** Application of 10 µmol/l Y15 significantly impaired FAK Y397-phosphorylation and induced cleavage of caspase-3 in in all three EwS cell lines in comparison to DMSO treatment. This was accompanied by a significant increase in apoptosis (ApoTox Glo Triplex assay, shown here are the results from A673 cells). **C,** ImageJ software-based analysis of fluorescence microscopy images showed that treatment of EwS cells with 10 µmol/l Y15 significantly decreased both number (left graph) and size (right graph) of Paxillin-positive focal adhesions (arrowheads) together with a loss of dorsal stress fibers (asterisks) in all three investigated EwS cell lines. **D,** Cell migration was significantly impaired upon treatment with 10 µmol/l of Y15 compared to DMSO in A673, TC-32 and CADO-ES1 cells. **E**, Reduction in migratory capacity of A673 cells upon application of 10 µmol/l Y15 occurred in parallel with a significant decrease in active Rho levels as shown by Rho activity pulldown assay.

Figure 3. Effects of Y15 treatment on EwS viability and invasion in an *in vivo* (avian CAM) model. A, Application of 10 µmol/l Y15 to A673 EwS cells 24h prior to cell seeding significantly impaired the rate of tumor formation as well as tumor size in the CAM model (p=0.0122 and p=0.0095, respectively) while not altering the (micro-)vascular architecture of the CAM. **B,** Histological analyses showed tumor regression, necrosis (**N**) and microcalcification with only very few residual tumor cells detectable (**arrowhead**) upon Y15 treatment. Immunohistochemistry and quantification via reciprocal intensity showed persistent expression of FAK in both, Y15-treated and control cells, but a significant decrease of FAK Y397-phosphorylation in the residual A673 xenograft tumor cells after treatment with Y15. **C,** Schematic diagram of how EWSR1-FLI1-dependent expression of Ezrin may contribute to SRC-independent autophosphorylation of FAK on tyrosine 397 as previously described.

473 The phosphorylation of FAK impairs apoptosis and anoikis and enhances focal adhesion formation
474 and migratory capacity of EwS cell, but can effectively be targeted by application of Y15.

475 **Supplementary Figure 1. A,** Detection of EWSR1-FLI1 and EWSR1-ERG fusion proteins in TC-32, A673
476 and CADO-ES1 cells. **B,** siRNA-based knockdown of Ezrin in TC-32 (48h) and CADO-ES1 (48h and 72h,
477 respectively). **C,** Compared to TC-32 and CADO-ES1, A673 showed the highest proliferative activity
478 and migratory potential in real-time proliferation and migration assays using the xCelligence system.
479 **D and E,** Software-based image analysis (ImageJ) showed numerous Paxillin-positive focal adhesions
480 (FA) in the investigated EwS cell lines, with the highest number of FAs observed in A673 and CADO-
481 ES1. **F,** FA protein expression in EwS cells. Strong expression and Y397-phosphorylation of FAK in all
482 investigated EwS cell lines, while FAK Y576/577 expression was only barely detectable. Y118-
483 phosphorylation of Paxillin was present only in CADO-ES1 cells

484

485

486

487

Figure 1

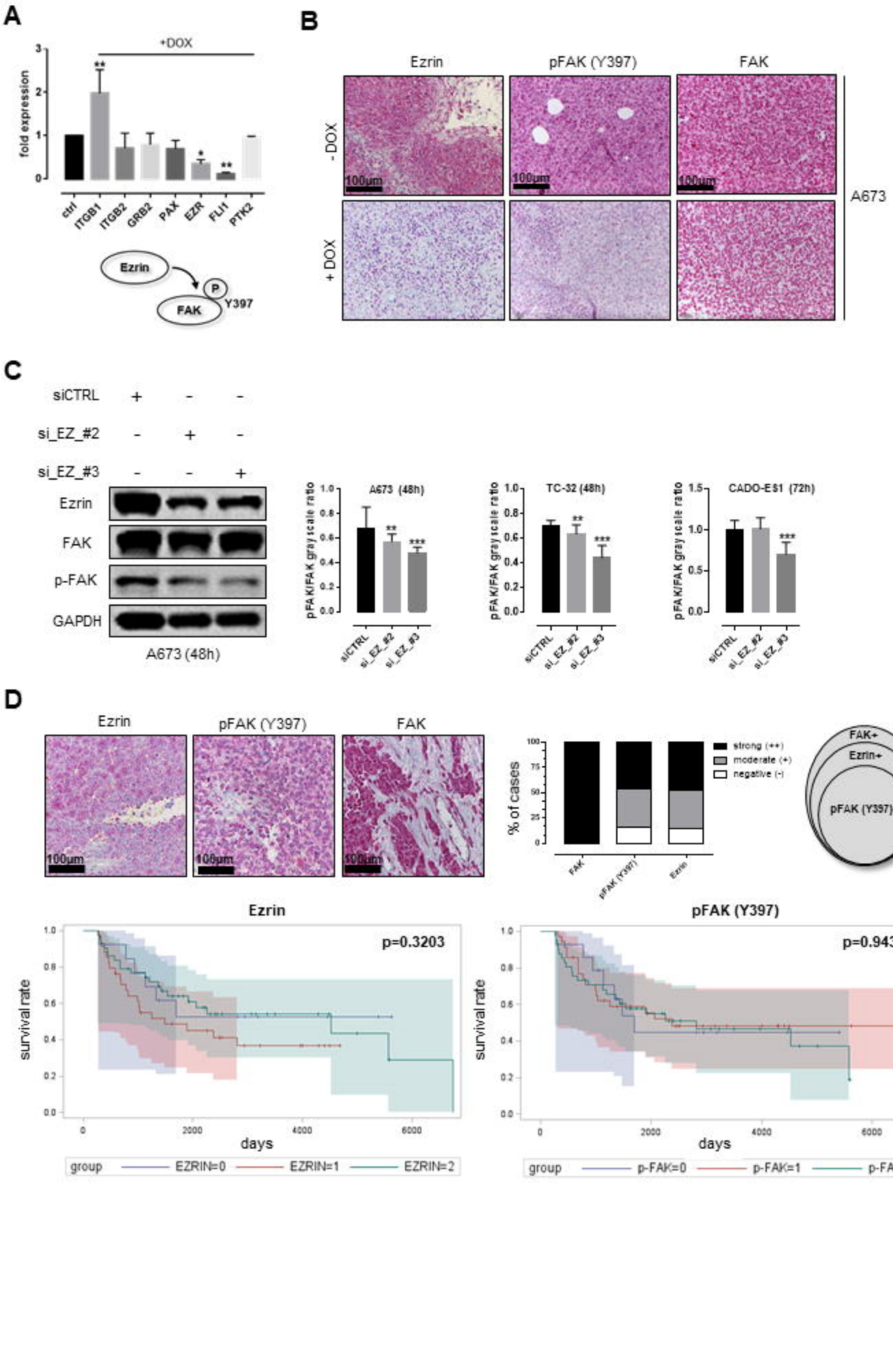

Figure 2

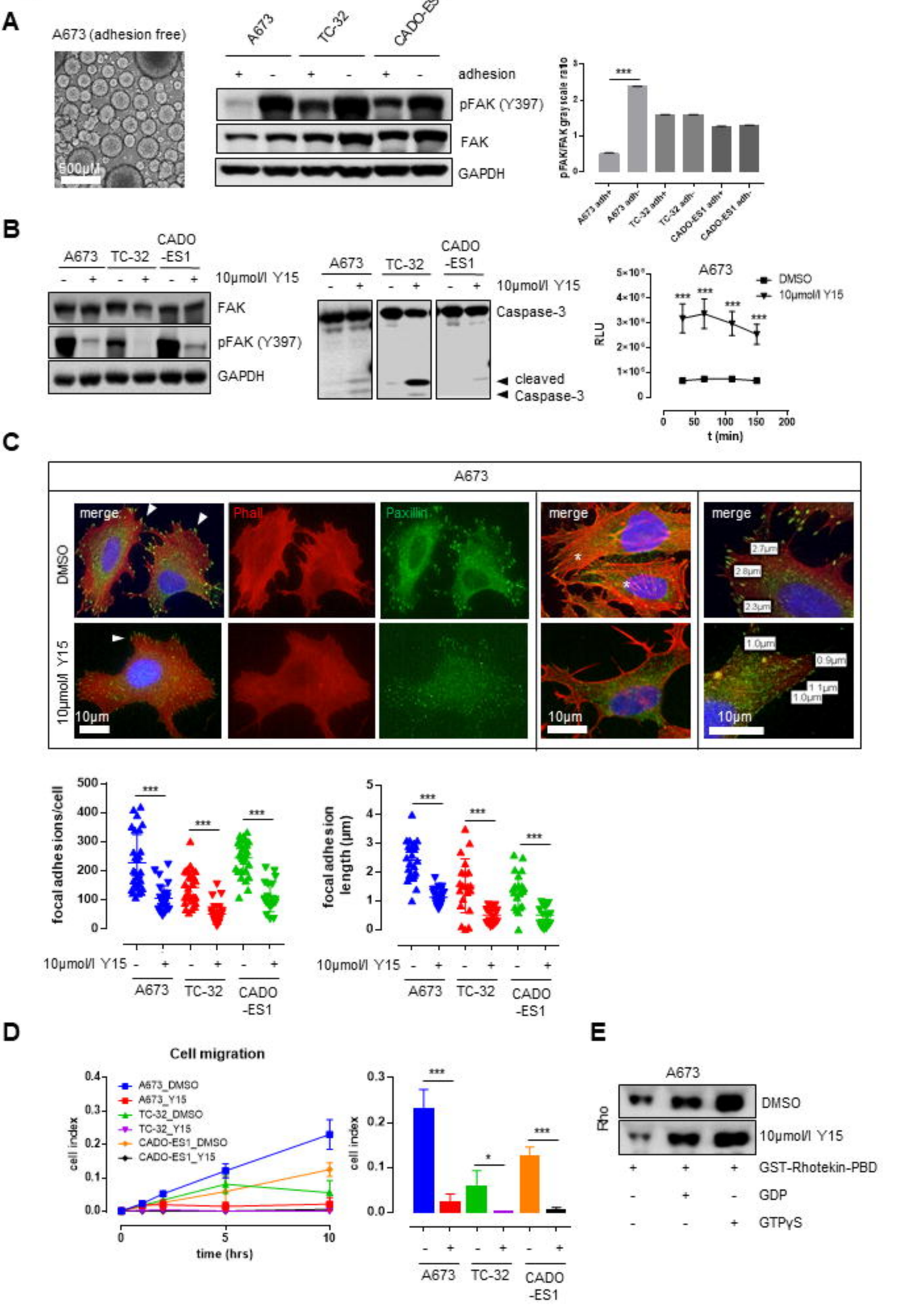

Figure 3